Mol Cell Biochem (2011) 352:143–154
DOI 10.1007/s11010-011-0748-y

Expression and analysis of two novel rat organic cation transporter homologs, SLC22A17 and SLC22A23

Katie M. Bennett · Jun Liu · Courtney Hoelting · James Stoll

Received: 2 April 2010 / Accepted: 17 February 2011 / Published online: 27 February 2011

Abstract The organic cation transporter (OCT, SLC22) family is a family of polyspecific transmembrane proteins that are responsible for the uptake or excretion of many cationic drugs, toxins, and endogenous metabolites in a variety of tissues. Many of the OCTs have been previously characterized, but there are a number of orphan genes whose functions remain unknown. In this study, two novel rat SLC22 genes, SLC22A17 (BOCT1) and SLC22A23 (BOCT2), were cloned and characterized. Northern blot analysis showed that BOCT1 and BOCT2 mRNA was expressed in a wide variety of tissues. BOCT1 was strongly expressed in brain, primary neurons and brain endothelial cells, with highest expression in choroid plexus. BOCT2 was also abundantly expressed in brain, as well as in liver. To characterize the products of these genes, BOCT1 cDNA was isolated from a rat blood–brain barrier cDNA library, and BOCT2 cDNA was isolated from rat brain capillary and from cultured neurons using PCR techniques. Plasmids expressing BOCT1 and BOCT2 were transfected into HEK-293 cells, as were control cDNAs for OCT1 and OCTN2. Recombinant cell surface protein was verified by western blot and fluorescence microscopy. Transport activity of BOCT1 and BOCT2 was evaluated using radioisotope uptake assays. The OCT1- and OCTN2-expressing cells transported the canonical substrates, 1-methyl-4-phenylpyridinium (MPP^+) and carnitine, respectively. However, BOCT1 and BOCT2-expressing cells did not show transport activity for these substrates or a number of other SLC22 substrates. These novel family members have a nonconserved amino terminus, relative to other OCTs, that may preclude typical SLC22 transport function.

Keywords BOCT · Membrane protein · Brain · Choroid plexus · Organic cation

K. M. Bennett · J. Liu · C. Hoelting · J. Stoll
Department of Biomedical Sciences, Texas Tech University Health Sciences Center, School of Pharmacy, 1300 S Coulter, Amarillo, TX 79106, USA

Present Address:
K. M. Bennett
Department of Laboratory Sciences and Primary Care, Texas Tech University Health Sciences Center, Lubbock, TX 79430, USA

J. Stoll (✉)
Department of Biomedical Sciences, Texas Tech University Health Sciences Center, School of Pharmacy, 1300 S Coulter, Amarillo, TX 79106, USA
e-mail: james.stoll@ttuhsc.edu

Introduction

The organic cation transporter (OCT) family (SLC22) is important for the uptake, reabsorption and excretion of drugs, nutrients, and metabolites. OCTs are ATP-independent facilitative transporters that are expressed in many tissues. These transporters are considered polyspecific in that they accept compounds with a variety of sizes and molecular structures. Functional and genetic analysis has provided evidence for three subclasses in the SLC22 family. The OCT subfamily (OCT1-3, SLC22A1-3) transports organic cations such as tetraethylammonium (TEA) and 1-methyl-4-phenylpyridinium (MPP^+). The OCTN subfamily (OCTN1-3, FLIPT1,2) transports zwitterions including carnitine. The OAT subfamily (OAT1-6, ORCTL3,4) transports a variety of organic anions and includes the transporters responsible for PAH/α-ketoglutarate exchange in the kidney [1]. In addition to these previously identified OCTs, the human and rodent genomes

have a number of SLC22 orphan genes whose functions remain to be identified.

The members of the OCT family are characterized by 12 putative transmembrane domains (TMDs), a large extracellular loop with multiple glycosylation sites between TMDs 1 and 2, an intracellular loop with phosphorylation sites between TMDs 6 and 7, and intracellular N and C-termini [2]. The known OCTs have been cloned from several species including human, rat, and mouse [3–10]. These transporters are conserved between species, indicating their importance for transport of organic cations. Mice in which the genes were disrupted confirm the role of these proteins in organic cation transport [11]. Several comprehensive reviews are available that detail the structure, function, and physiological roles of the OCTs [1, 12].

In this article, we report the cloning, tissue expression and initial characterization of two orphan genes in the OCT family, SLC22A17 (BOCT1) and SLC22A23 (BOCT2). These genes were identified by database searches for OCT-related genes and have also been identified by others using bioinformatic analysis [13, 14]. In the databases, SLC22A17 was termed BOCT (brain organic cation transporter) or BOIT (brain organic ion transporter) due to the fact that it was sequenced from a brain cDNA library. SLC22A17 was also recently identified as a possible receptor for lipocalin-2 [15]. We show that these proteins are molecularly related to the SLC22 family, although the sequences diverge in the N-terminal region. Neither protein was able to transport typical SLC22 substrates even though it was present on the cell surface. These results suggest evolution of the core structure of a typical membrane transporter family to adopt new physiological functions.

Experimental

cDNA Library construction and screening

A blood–brain barrier cDNA library was constructed from rat brain capillaries. The capillaries were purified by filtration on glass beads as previously described [16]. Total RNA was isolated from purified capillaries and polyA + RNA purified by oligo-dT chromatography. A cDNA library was constructed in λZAPII using a commercial kit. The unamplified library contained 1.1×10^6 independent clones.

The library was screened for BOCT1 by standard methods [17] using a [^{32}P]labeled cDNA fragment. The fragment was prepared by PCR amplification of rat brain capillary cDNA using primers 445, 446 (A listing of PCR primers is given in Table 1). Thirteen positive clones were obtained from a total of 250,000 screened. One clone, #12, contained an insert of 2.4 kb, similar to the size of BOCT1 mRNA detected on a northern blot of capillary RNA using the same probe. Clone 12 was sequenced, and the sequence matched the predicted sequence NM_177421 except that clone 12 lacked 7 nt at the 5′ end.

Table 1 PCR primer sequences

Primer	Sequence
B0CT1 primers	
445 (rat)	5′-AGTGAAGCGGCAGATTGAG-3′
446 (rat)	5′-CAGCTTGGGAGGAGAAGAG-3′
B0CT2 primers	
469 (rat)	5′-ATCCCGGCGCTGTTCATC-3′
470 (rat)	5′-CGGCTAGC C CA GGCAT GAGG-3′
476 (rat, 3′-RACE)	5′-GGCGGCGGCTACCAGAAGACCCTG-3′
477 (rat, 5′-RACE)	5′-GGGACAGATGATGAGGGCCTGCAA-3′
482 (rat, 3′-RACE)	5′-TGAGGCCAGGGCAGTGAGGATCATG-3′
489 (rat)	5′-AGCGCCCGAAGT CCGTGGAG-3′
490 (rat)	5′-CGCG GCC GGAGA GAATG CTC-3′

Primers were designed for BOCT1 and BOCT2 for RT-PCR analysis and for RACE PCR cloning of BOCT2

The cDNA library was also screened for BOCT2. The probe was a labeled PCR fragment obtained by amplification of capillary RNA with primers 469, 470. The library was screened three times but no positive clones were identified. However, a northern blot containing the same RNA preparation clearly demonstrated a hybridizing mRNA. We believe BOCT2 was not present in the cDNA library because GC-rich secondary structure (see below) at the 5′ end precluded its inclusion in the library.

Isolation of SLC22A23 cDNA by RACE

To isolate a full-length BOCT2 cDNA, RACE (rapid amplification of cDNA ends) was performed using the BD Smart RACE cDNA Amplification Kit (BD Biosciences) using RNA purified from rat brain cultured primary neurons (see Fig. 3 for the location of primers used in RACE).

3′ RACE with the internal primer 469 yielded two main bands of 2 and 5 kb. The 2 kb sequence began with primer 469 and extended to a polyadenylation sequence and short polyA stretch that is 265 nt downstream of the predicted stop codon. The 2 kb RACE clone has a bona fide 3′ terminus and thus corresponds to the 3 kb mRNA observed on the northern blot. The sequence of the 2 kb clone matched the database sequence XM_341519 over this stretch. The 5 kb RACE fragment was not further analyzed but presumably corresponds to the 6 kb mRNA.

To obtain the 5′ end of BOCT2, PCR required the use of GC-rich conditions. This is because the 5′ end of the BOCT2 mRNA is ~80% GC. We did not obtain a genuine 5′ RACE product using routine conditions. Amplification conditions were 30 cycles of: denaturation, 30 s 94°C,

annealing 30 s 55°C, 2 min 72°C, in the presence of GCmelt (BD Biosciences). The 5′ region was amplified with either primers 489/482 or 489/490. Primer 489 was not part of XM_341519 and was chosen from the rat genomic sequence to give the mRNA size observed on northern blots. The predicted 1.9 kb DNA was obtained upon amplification with primers 489/482. As this DNA crosses multiple splice sites, amplification of this band cannot result from genomic DNA and therefore it represents the actual mRNA. The 1.9 kb band was only obtained when PCR was performed under GC-rich amplification conditions. In routine PCR buffers, low yields of shorter fragments were obtained that contained variable deletions in the GC-rich sequence, presumably a result of skipping through secondary structure in this region. A full-length BOCT2 cDNA was assembled by fusing the 482/489 cDNA with the 3′RACE cDNA at an internal MluI site.

Northern blot

A multi-tissue northern blot was obtained commercially (Ambion) to measure expression in generic tissues in the body. To test for expression in specific tissues, RNA was isolated by Trizol (Invitrogen) and blots were prepared on nylon membranes using total RNA according to routine methods [17]. Probes were prepared by random primer labeling of PCR fragments. BOCT1 expression was identified with the DNA generated by primers 445/446. BOCT2 expression was measured with either a DNA produced by primers 469/470 or 489/490. Blots were hybridized overnight at 45°C in Hybrisol I and washed at a stringency of 0.2× SSC, 0.5% SDS at 55°C. Hybridized bands were detected and the data captured by Molecular Imager FX (Biorad).

Expression cloning and analysis

PCR-amplified cDNAs of BOCT1 and BOCT2 were subcloned into the p3X-FLAG-CMV-10 expression vector (Sigma). Alternatively, BOCT1 and BOCT2 were expressed with N-terminal myc epitopes by cloning cDNAs into pCMV-3Tag2 (Stratagene). In the BOCT1-FLAG construct, the cDNA contained 24nt of the 5′UTR. In the BOCT2-FLAG construct, the entire 5′UTR beginning with primer 489 was present. A truncated BOCT2-Flag construct was also generated that began with the second in-frame AUG (aug* in Fig. 3). For cloning of BOCT1 and BOCT2 into pCMV-3Tag-2, the coding region from initiator to stop codon was amplified and inserted downstream of the N-terminal Myc sequence. For OCT1 and OCTN2, the coding regions of these cDNAs were amplified from mouse kidney cDNA by PCR and cloned into p3X-CMV-FLAG or pCMV-3Tag-2. All plasmids were verified by DNA sequencing. For stable transfections, the plasmids were linearized and transfected into T-REx-293 cells (Invitrogen) using Lipofectamine 2000 (Invitrogen). G418 (1 mg/ml) was added to the medium [DMEM:F12 (1:1), 10% FBS] on day three after transfection to select for plasmid-containing cells. After selection of resistant colonies, cells were routinely maintained in 0.5 mg/ml G418.

Cell surface protein expression was verified by biotinylation. Cells were incubated with membrane-impermeable sulfo-biotin (Pierce) according to manufacturer's instructions. Biotinylated proteins were purified from cell lysates by streptavidin chromatography and the fusion protein detected by western blot using anti-FLAG M2 monoclonal antibody (Sigma). Each blot was then stripped and re-incubated with anti-GAPDH antibody (Chemicon International, MAB374) to illustrate that intracellular protein did not bind inadvertently to streptavidin. For detection by fluorescence microscopy, cells were fixed, permeabilized, and incubated with anti-FLAG M2 monoclonal antibody, followed by a fluorescent anti-mouse antibody (Alexa Fluor 488, Invitrogen).

Transport assays

Cells were plated in 35 mm dishes or 96 well plates and assayed for uptake of radiolabeled substrates (from Perkin-Elmer or American Radiolabeled Chemical). Cells were washed with prewarmed balanced salt solution (BSS, 10 mM HEPES, 1.8 mM CaCl, 5.3 mM KCl, 0.8 mM $MgSO_4$, 120 mM NaCl, 1 mM $NaPO_4$, 5.6 mM glucose, pH 7.4) at 37°C. The wash was replaced by BSS containing 1 μCi/ml radiolabeled substrate: [^{3}H]choline (80 Ci/mmol), [^{3}H]carnitine (80 Ci/mmol), [^{3}H]TEA (20 Ci/mmol), [^{3}H]MPP^+ (85 Ci/mmol), [^{3}H]nicotinamide (25 Ci/mmol), [^{3}H]norepinephrine (44.6 Ci/mmol), [^{3}H]histamine (12.5 Ci/mmol), [^{14}C]urate (54 mCi/mmol), or [^{14}C]ascorbate (5.4 mCi/mmol). Uptake was measured in triplicate at 37°C for 3 min (choline and MPP^+), 15 min (carnitine), 30 min (TEA), or at 21°C for 1 h (nicotinamide, NE, histamine, urate, ascorbate). The dishes were transferred to ice and immediately washed 3–4 times with ice cold PBS. Cells were solubilized with 0.4 M NaOH. Aliquots were taken to measure radioactivity and protein. The results are expressed as dpm/μg of protein (mean ± SD) or as percent of control. Statistical significance was assessed by ANOVA and Bonferroni multiple comparison test.

Results

Expression of BOCT1 and BOCT2 mRNA

Two predicted but previously uncharacterized rat genes, which are most related to the SLC22 family, are present in

NCBI databases. These two genes encode transporters SLC22A17 (NM_177421) and SLC22A23 (XM_341519). We focused on rat sequences, but similar predicted proteins were identified in human and mouse genomes. SLC22A17 was termed BOCT (or BOIT) in the databases. SLC22A23, when analyzed by ClustalW, is most similar to SLC22A17 and therefore we refer to them as BOCT1 and BOCT2. These orphan sequences were most similar to the OCT subfamily of SLC22 when analyzed by ClustalW. To verify that orphan genes are expressed and not simply pseudogenes, RT-PCR was performed. cDNAs were prepared from several different tissues and cultured cell lines [rat brain capillaries, mouse kidney, A549, MC-IX-C, NG-108] and amplified using primers derived from the predicted sequences. PCR products were obtained from nearly all the cDNAs and verified by DNA sequencing, thus confirming that these predicted genes were expressed. A commercially available multi-tissue northern blot was then probed with radiolabeled PCR products (Fig. 1). The blot hybridized to BOCT1 cDNA showed a major band at 2.5 kb (Fig. 1a). Expression was highest in brain, exceeding that of all other samples on the blot. Kidney and liver showed intermediate levels of expression whereas lower expression was observed in heart, stomach and testis. When the blot was probed for BOCT2 expression, a more complicated pattern was seen (Fig. 1b). Most tissues showed three hybridizing bands of 6, 4.2 and 3.0 kb, with the 6 kb band typically, but not always, showing the highest labeling. The weak 2 kb band in testes was seen only on this blot and not others. BOCT2 was expressed in most tissues but with a range of abundances. The highest levels were observed in liver, brain, kidney, and spleen. Lower levels were observed in skin, lung, and intestine. Expression was low in the remaining tissues. Neither BOCT1 nor BOCT2 is expressed strongly in muscle. RACE experiments suggested that the multiple BOCT2 mRNA bands are likely due to alternative polyadenylation.

Expression was further analyzed on a blot containing RNA from various cultured cells or tissue samples not present on the commercial blot (Fig. 2). The most significant finding was robust expression of BOCT1 in choroid plexus, higher than in whole brain, indicating that BOCT1 is enriched in choroid plexus. BOCT1 was also highly expressed in cultured neurons and at lower levels in cultured astrocytes. Hybridization to capillary RNA in Fig. 2 was weak perhaps due to RNA degradation in the sample on this blot. However, expression in brain capillaries at levels comparable to whole brain was demonstrated by RT-PCR and in other blots (not shown). Also, BOCT1 cDNA was cloned from a brain capillary cDNA library thus confirming its expression in this tissue. Thus, BOCT1 is widely expressed in brain and is not limited to the barriers. Expression of BOCT1 was also seen in NG108 neuroblastoma and C6 astroglioma cell lines, but was barely detectable in MC-IX-C neuroblastoma or bEnd5 endothelial cell lines (Fig. 2). BOCT1 can, however, be detected in MC-IX-C by the more sensitive RT-PCR technique (not shown).

BOCT2 was not detected in choroid plexus, in contrast to BOCT1 (Fig. 2). The highest level was observed in RNA

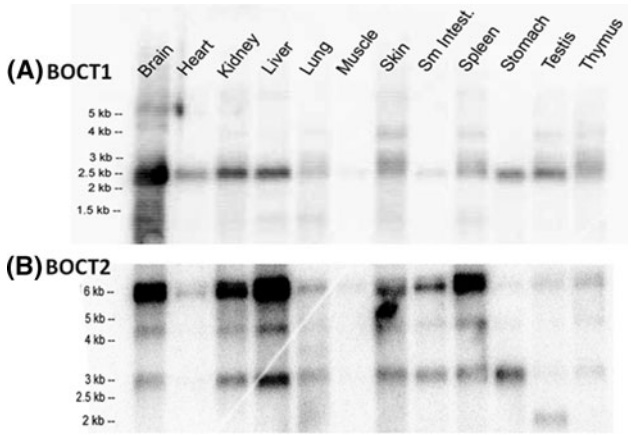

Fig. 1 BOCT1 and BOCT2 are expressed in a variety of tissues. A multi-tissue northern blot was obtained commercially (Ambion) to measure mRNA expression in generic tissues in the body. Probes for BOCT1 (**a**) and BOCT2 (**b**) were prepared by random primer labeling using PCR fragments described in methods for library screening. Blots were hybridized overnight at 45°C in Hybrisol and washed at a stringency of 0.2× SSC, 0.5% SDS at 55°C. Hybridized bands were detected and the data captured by phosphoimaging

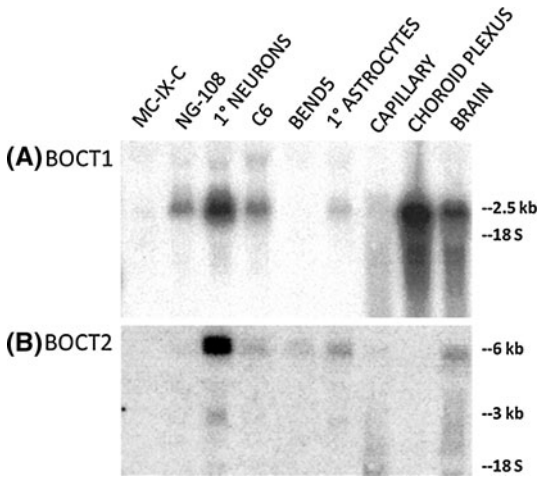

Fig. 2 BOCT1 and BOCT2 expression in choroid plexus and cell lines. Total RNA was isolated from the indicated tissues and cell lines and a northern blot was prepared. Probes were prepared for BOCT1 (**a**) and BOCT2 (**b**) by random primer labeling using PCR fragments described in methods for library screening. Blots were hybridized overnight at 45°C in Hybrisol and washed at a stringency of 0.2× SSC, 0.5% SDS at 55°C. Hybridized bands were detected and the data captured by phosphoimaging

from primary cultured neurons. Lesser expression was observed in whole brain, primary astrocytes, as well as bEnd5 and C6 RNA. Hybridization to capillary RNA was seen on other blots, at a level comparable to whole brain RNA. BOCT2 was barely detectable in either MC-IX-C or NG108 neuroblastoma although it was detectable in these cell lines by RT-PCR.

BOCT1 and BOCT2 cDNAs

We wanted to understand the role that BOCT1 and BOCT2 might play in transporting organic ions into and out of brain. As the initial step, a rat blood–brain barrier (BBB) library was screened to isolate cDNAs for the two genes. The sequence for BOCT1 had been assembled from ESTs but a full-length cDNA was not independently reported. Furthermore, BOCT2 was derived primarily from gene prediction analysis and present in the databases as a partial sequence. Thus, it was important to verify that the assembled database sequences represented the actual tissue mRNA sequences.

Multiple BOCT1 cDNA clones were isolated from a rat brain capillary library. The largest clone was 2,368 bp. Given that northern analysis revealed an mRNA size of 2.5 kb, this clone is essentially full-length. When the DNA sequence was compared to the predicted database sequence NM_177421, they were identical except that the BBB clone was 7 nt shorter at the 5′-end and contained a 19 nt polyA tail. Smaller clones from the library screening were fragments of the larger clone. There was no evidence of alternatively spliced exons in this cDNA library. Sequence analysis revealed an open reading frame that yields a protein of 516 amino acids. A long 5′UTR of 457 nt is predicted. The 5′UTR contains an open reading frame of 137 codons beginning 280 nt upstream of BOCT1 that overlaps the beginning of the protein. A search of rat protein databases with the predicted upstream protein yielded no similar sequences. The presence of this upstream ORF suggests BOCT1 may be subject to translational regulation.

When the BBB library was screened for BOCT2, no positive clones were identified. This occurred even though RT-PCR and northern analysis clearly showed the expression of this gene in brain capillary RNA. To isolate a cDNA, RACE was performed using cDNA from primary cultured neurons, in which BOCT2 is abundantly expressed. Figure 3 shows a model of the 3 kb mRNA sequence that resulted from RACE along with the position of the primers that were used. The long ORF encodes a protein of 689 amino acids. The 3 kb mRNA has a short 265 nt 3′UTR that ends with a poly A signal and a polyA tail. The larger mRNAs observed on northern blot extend through this polyA signal. The 5′UTR is ~80% GC and this GC-rich region extends into the ORF approximately 300 nt downstream of the putative start codon. Analysis of the BOCT2 sequence by mFOLD predicted significant secondary structure in the GC-rich region. In particular, two perfect 23 bp inverted repeats are present beginning 240 and 60 nt upstream of the first AUG (Fig. 3). Evidence of complex structure was provided by PCR experiments. RT-PCR of neuronal cDNA using primers 489/482 yielded the expected 1.9 kb DNA only when performed under GC-rich conditions (Fig. 3). Under generic conditions amplification was weak and only smaller size products were obtained (Fig. 3, left lanes). Even under GC-rich conditions, a truncated 1.7 kb DNA was obtained. Amplification was unaffected using primers (476/482) outside the repeat region (Fig. 3, lanes 3). Cloning and sequencing of these shorter products showed deletions of the GC-rich region that always included the inverted repeats. The deletions had different start and stop points, which means the shorter fragments are not simply splice isoforms and are due to skipping regions of secondary structure during amplification. RT-PCR using primers 489/490 yielded similar results in that a product was obtained only in conditions that melt GC-rich DNA (Fig. 3, lanes 1). Primer 490 is located between the inverted repeats and this data supports the presence of a stem-loop structure. When the 489/490 PCR product was hybridized to the blot used in Fig. 1, the same three mRNA bands were detected as seen with the 469/470 probe (data not shown). This result confirms the presence of the inverted repeats in BOCT2 mRNA. A defined 5′ end was not observed in these experiments. Whether this was due to difficulties amplifying GC-rich sequences, or that this gene simply shows heterogeneity of transcription initiation is unknown. However, transcription initiation begins within 100 nt of primer 489 based on the size of BOCT2 mRNA on blots. The predicted initiator AUG is present in the GC-rich region and is located 40 nt downstream of the second repeat. The next in-frame AUG (aug* in Fig. 3) is 444 nt downstream and is outside the GC-rich sequence. However, aug* is not likely to be the initiator codon, because a FLAG-tagged ORF beginning with aug* did not yield a protein product when expressed in cells. Based on the first AUG a 5′UTR of at least 350 nt is calculated. The 5′UTR contains the inverted repeats suggesting the possibility of a regulatory stem-loop structure upstream of the translation start site. One example of alternative splicing was discovered for BOCT2. The predicted amino acid sequence was 8 amino acids shorter in rat capillary cDNA than in neuronal cells. This was due to selection of a 3′ splice site 24 nt downstream of the splice site used in neuronal cells. The amino acid insert begins at aa522(Gly) in the loop between TM9 and TM10 (see Fig. 4).

Sequence analysis of BOCT1, BOCT2, and comparison with OCTs

The predicted amino acid sequences for BOCT1 and BOCT2 were compared to other members of the SLC22

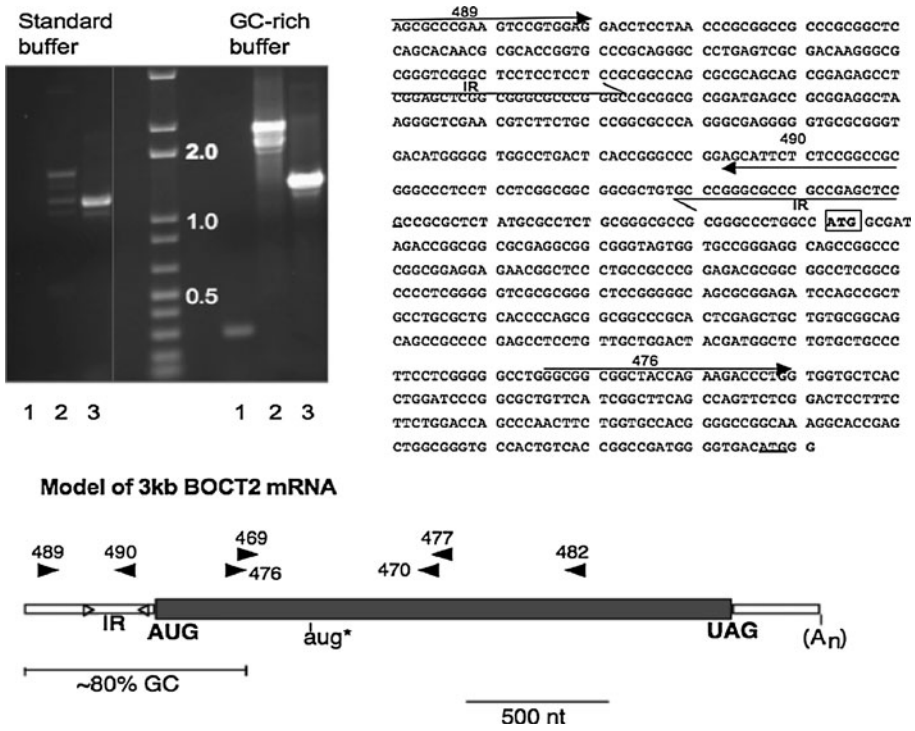

Fig. 3 Structure of BOCT2 mRNA. RT-PCR: (*Top left*) Rat primary cultured neuron cDNA was amplified under generic or GC-rich PCR conditions and analyzed by agarose gel electrophoresis. *Lane 1*: Primers 489/490. *Lane 2*: Primers 489/482. *Lane 3*: Primers 476/482. *M*: DNA standards. (*Top right*) Sequence of the 5′ end of BOCT2 mRNA from primer 489 to downstream AUG. PCR primers are indicated with *arrows*. 23 bp indirect repeats are indicated with *half-arrow*. Initiator AUG is boxed in bold. Second AUG is underlined. Examination of the sequence shows its GC-rich nature. (*Bottom*) A model of the BOCT2 3.0 kb mRNA is illustrated. Primer sites used for PCR are indicated with *arrowheads*. The predicted ORF is *shaded*. Location of the inverted repeats (IR) in the 5′UTR is shown with *triangles*

family (Fig. 4). The BOCT sequences were more similar to each other (34% identity) than to other SLC22 gene products. Both, however, showed significant similarity to all known SLC22 members. BOCT1 was most similar to the following SLC22 members: BOCT2 > OCT3 > OCT1 > OCT2 > ORCTL3. BOCT2 was most similar to BOCT1 > OCT3 > ORCTL3 > OCTN3 > OAT2. An alignment of BOCT sequences with selected SLC22 members is shown in Fig. 4. Transmembrane sequences were predicted by TOPCONS [18] and are shown in the figure for reference purposes.

Sequence similarity between the BOCT proteins and other members of the SLC22 family extends from upstream of TM2 through TM12. However, the N-terminal sequences of the BOCTs showed no similarity with other SLC22 proteins, beginning approximately 30 residues upstream of TM2. Of significance, several conserved motifs in the SLC22 family are observed in the BOCT proteins. These motifs include the AFS motif on the N-terminal side of TM2, the MFS motif located between TM2 and TM3 [19], and a highly conserved motif (ELYPTVIR) between TM10 and TM11. Also, sequence conservation is observed at the cytoplasmic ends of TM6 (PESXRWL) and TM12 (LLPETKXXXLPETI). Similar to the other SLC22 proteins, the BOCT proteins are divided in two halves by a 60–70 amino acid cytoplasmic loop. This loop contains several canonical sites for phosphorylation by PKC or PKA. Interestingly, a residue in TM11 previously shown to be critical for ion specificity [20], R472 in OAT2, D473 in OCT3, is a neutral residue in the BOCT proteins (A437 in BOCT1, G575 in BOCT2). Finally, both BOCT proteins show a possible diLeu motif in the C-terminal tail (aa508–513 in BOCT1, aa643–647 in BOCT2).

The greatest difference between the BOCTs and the rest of the SLC22 family is at the N-terminus. At 516 residues, BOCT1 is shorter than the typical SLC22 protein, and the size difference is due primarily to a shorter N-terminus. The typical SLC22 protein contains a cytoplasmic N-terminus and a larger, ~100 amino acid, glycosylated extracellular loop between TM1 and TM2. BOCT1 does not show a comparable TM1 domain. In fact, N-terminal of the AFS motif (aa 84–94 in BOCT1), there is no homology between BOCT1 and other family members. There are two N-linked glycosylation sites at residues 23 and 32, and least one of these is glycosylated as inferred from PNGase F sensitivity (data not shown). This indicates that the N-terminus is extracellular in BOCT1.

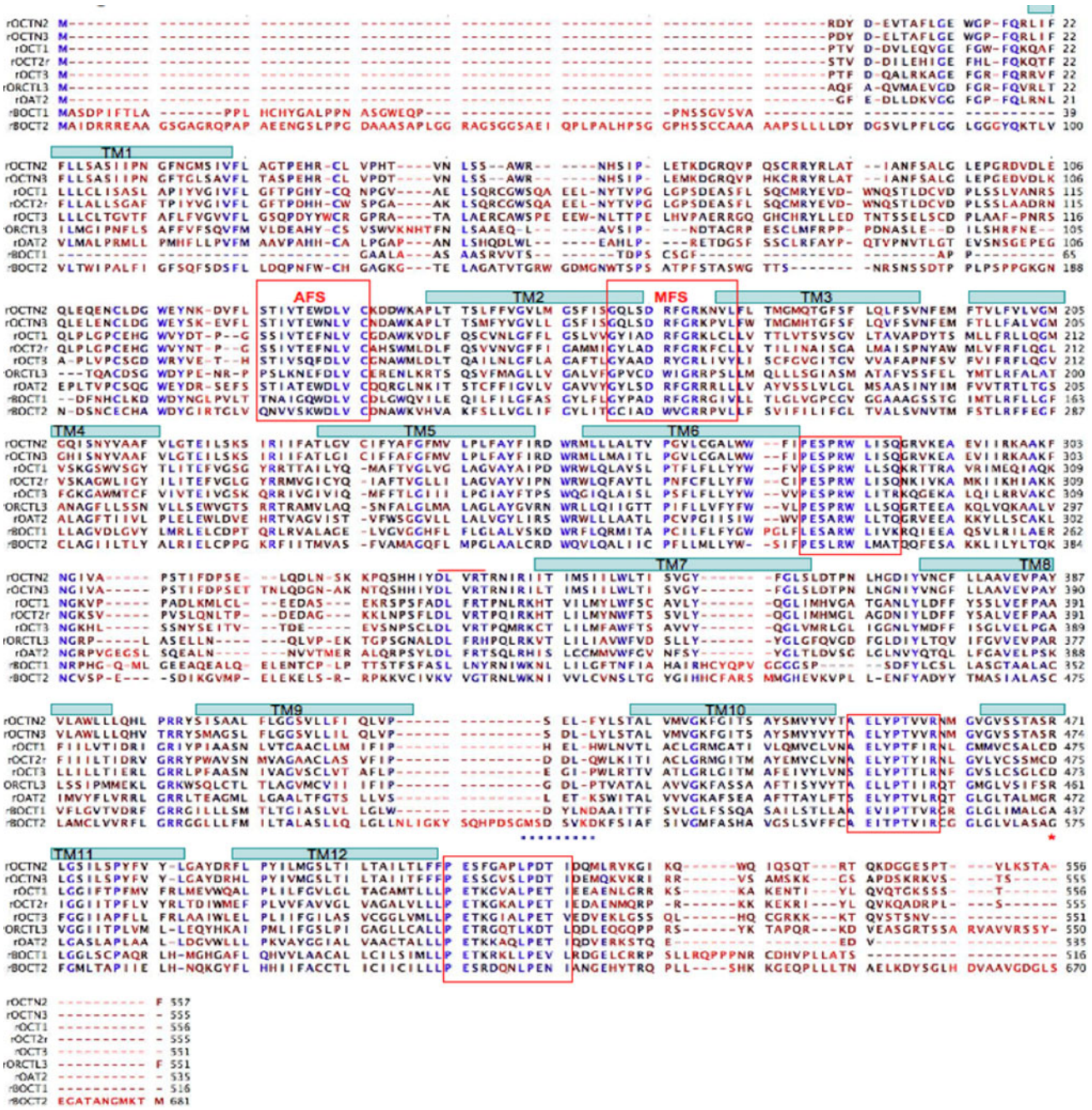

Fig. 4 BOCT sequence alignments. The rat SLC22 sequences listed were aligned using T-COFFEE (CLCbio). Highly conserved residues are colored blue, moderately conserved residues are *black*, nonconserved residues are *red*. TMDs were predicted using TOPCONS and are illustrated as blue rectangles overlying the TMD sequence. Highly conserved motifs are boxed in red. The 8 amino acid insert (GMSDSVKD) is underlined with a *dotted blue line*. The ion specificity residue in TM11 is marked with a *red* asterisk (*) OCTN2 (SLC22A5); OCTN3 (SLC22A9); OCT1 (SLC22A1); OCT2 (SLC22A2); OCT3 (SLC22A3); ORCTL3 (SLC22A13); OAT2 (SLC22A7). See online article for color version of this Figure

In contrast, BOCT2 is significantly larger (681aa) than the typical SLC22 protein. Similar to BOCT1, this extra protein sequence is upstream of the AFS motif and shows little homology to other SLC22 members. Topology software predicts only a weak TM1 segment (0.6 probability) although it occurs in a position analogous to TM1 of other OCTs. If this segment is correct, it predicts a 97 amino acid intracellular N-terminus (~20 residues in other SLC22's). There are 5*N*-linked glycosylation sites at residues 24, 151, 170, 173, and 189, although the site at aa24 is predicted to be intracellular in the 12-TMD model. Another second, less favored topology predicted by TopPredII has 13 TMDs.

In this model, two TMDs (aa72–92, 96–116) form a hairpin in the region corresponding to TM1. This model predicts an extracellular N-terminus. The actual membrane topology for BOCT2 awaits experimental evidence.

Functional expression

To express the BOCT1 and BOCT2 proteins for functional analysis, the cDNAs were subcloned into the p3X-CMV-FLAG plasmid expression vector, which allowed tracking of the recombinant proteins using a monoclonal anti-FLAG antibody. As positive controls for uptake assays, the OCT1 and OCTN2 coding regions were also expressed in a similar fashion. After cloning and sequence confirmation, the plasmids were stably transfected in HEK-293 cells.

Cell surface recombinant protein expression was first measured by biotinylation of cell surface proteins followed by purification using streptavidin chromatography. The lysates were analyzed by western blot using anti-FLAG antibody. Western blot of biotinylated protein fractions showed that all four recombinant proteins reached the cell surface (Fig. 5), as indicated by a band in the lanes containing purified, biotinylated protein (CS). The size of each protein was greater than the predicted amino acid sequence, consistent with glycosylation. As predicted, BOCT1 was smaller than OCT1 and OCTN2, which were smaller than BOCT2. The lysates from pBOCT2-FLAG and pOCT1-FLAG expressing cells showed a pair of bands. The lower molecular weight band in these samples may represent immature protein since it was underrepresented on the cell surface. The immunoblots were subsequently assayed for the intracellular protein, GAPDH. GAPDH was not present in the CS fraction, demonstrating that intracellular proteins were not labeled. This indicates that BOCT proteins in the CS fraction represent actual cell surface protein and not intracellular transporter that was incorrectly biotinylated.

Recombinant protein expression was also evaluated by fluorescence microscopy. In agreement with the western blot analysis, recombinant protein was found on the cell surface and in the cytoplasm (Fig. 5). Intracellular BOCT1 protein was localized in a punctate distribution. In contrast, in BOCT2, OCT1, and OCTN2 transfectants, intracellular staining was diffuse. Independent BOCT1 clones varied in the proportion of FLAG-tagged protein on the cell surface with as much as 50% cell surface expression in some clones. However, even in clones with the highest cell surface expression, BOCT1 still showed vesicular intracellular staining. It is inferred that the heterogeneous distribution of BOCT1 may be important for its function. In sum, the conclusion from these experiments is that the proteins are reaching the cell surface, a necessary prerequisite for measuring cellular uptake of organic ions by the proteins.

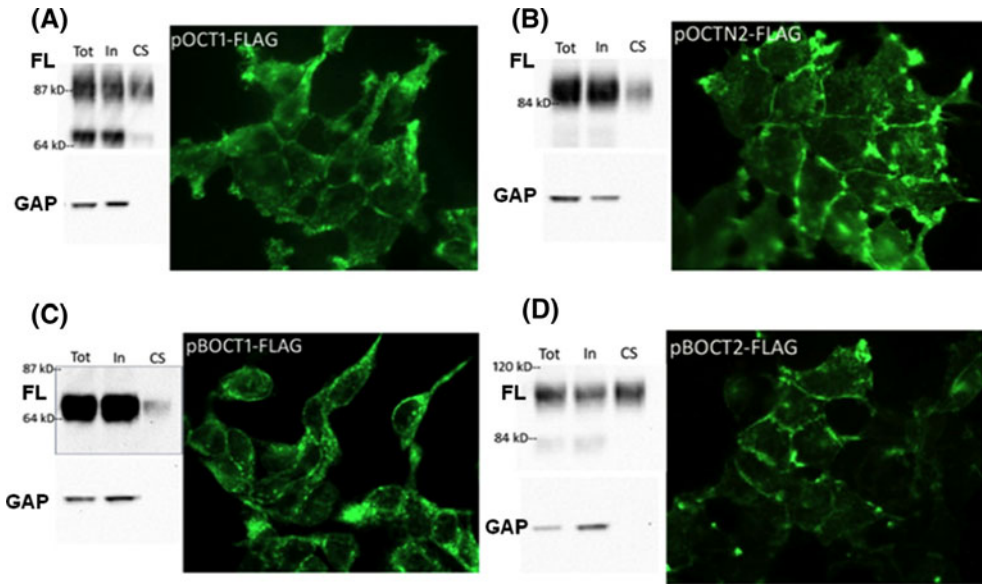

Fig. 5 Recombinant BOCT1 and BOCT2 protein is expressed on the cell surface. Stable recombinant HEK cell lines were analyzed for expression of FLAG fusion protein by immunofluorescence and by western blot. **a** pOCT1-FLAG, **b** pOCTN2-FLAG, **c** pBOCT1-FLAG, **d** pBOCT2-FLAG. Each panel is a composite of the biotinylation experiment (*left*) and cell staining (*right*). *Left*: Cells were incubated with membrane-impermeable sulfobiotin and biotinylated proteins purified on streptavidin beads, followed by western blot analysis using anti-FLAG antibody (*upper blots*, FL). Each lane contains protein from an equivalent amount of starting material. *Tot* total protein before purification, *In* intracellular protein (non-biotinylated), *CS* cell surface protein (biotinylated). Blots were stripped and incubated with anti-GAPDH to verify that only cell surface protein was purified (*lower blots*, GAP). *Right*: Stable transfectants in culture were fixed with paraformaldehyde, permeabilized, and immunostained with anti-FLAG followed by fluorescent secondary antibody

Transport assays

Functional activity of BOCT1 and BOCT2 was evaluated using radioisotope transport assays. Uptake of organic cations was measured in BOCT1, BOCT2, OCT1, and OCTN2-expressing HEK-293 cells and compared to cells containing the empty p3X-CMV-FLAG plasmid vector. Uptake of the prototypical OCT substrate MPP^+ was assayed in HEK transfectants with pOCT1-FLAG cells serving as a positive control. As expected, the OCT1-expressing cells transported 40-fold more MPP^+ (372 ± 12 dpm/μg) than vector-only cells (9.3 ± 0.8 dpm/μg). However, MPP^+ uptake by BOCT1 and BOCT2-expressing cells was not different than controls (Table 2). Two other organic cations, TEA and choline, were tested for transport and yielded identical results. That is, OCT1-expressing cells showed enhanced uptake of these compounds while BOCT1- and BOCT2-expressing cells were no different than control. The zwitterion, carnitine, a typical substrate for the OCTN subfamily was then tested. OCTN2-expressing cells showed 12-fold greater uptake than control (2,288 vs. 186 dpm/μg). However, carnitine uptake was unaffected by BOCT1 and BOCT2 expression as was the uptake of another zwitterion, the cationic amino acid, arginine. Accumulation of the fluorescent cation, ethidium, was also measured in SLC22-expressing cells. Whereas OCT1-expressing cells accumulated more ethidium relative to vector-containing cells (OCT1: 1,375 ± 328 FU/μg; vector: 35 ± 2 FU/μg), there was no statistically significant increase in ethidium accumulation in either BOCT1 or BOCT2-expressing cells (BOCT1: 52 ± 5 FU/μg; BOCT2: 48 ± 10 FU/μg).

Although MPP^+ is a substrate for nearly all the cation-transporting members of SLC22, it is possible that BOCT1 and BOCT2 have a more restricted substrate profile than other polyspecific members. Therefore, several other substrates were tested for transport activity. Of the SLC22 members, BOCT1 and BOCT2 showed the greatest similarity to OCT3 and ORCTL3. OCT3 (SLC22A3) was previously identified as the extraneuronal monoamine transporter and transports a variety of neurotransmitters including norepinephrine, serotonin, and histamine [21]. Based on this homology, we tested the BOCT's for neurotransmitter transport. Although we could show transport of histamine and norepinephrine in OCT1-expressing cells, there was no evidence for transport of these compounds by either BOCT1 or BOCT2 (Table 2). ORCTL3 (SLC22A13) was recently deorphanized and shown to transport nicotinate, para-aminohippurate (PAH), and urate [22]. Cells expressing BOCT1, BOCT2, or OCT1 were unable to accumulate urate relative to vector-containing cells (Table 2). Furthermore, to test if the BOCT proteins were behaving as anion transporters, the uptake of PAH and ibuprofen was assayed. Neither drug was transported by BOCT1 or BOCT2 (data not shown). As final candidate substrates, the transport of nicotinamide and ascorbic acid was tested. BOCT1 was abundantly expressed in choroid plexus, which is a major site of vitamin transport in the brain. In fact, an ascorbate transport activity has been identified in choroid plexus, for which the transporter involved has not been identified [23]. However, ascorbate or nicotinamide uptake in BOCT1 or BOCT2-expressing cells was not significantly different than in vector-containing cells. OCT1-containing cells accumulated nicotinamide but not ascorbate (Table 2).

To rule out the possibility that the C-terminal FLAG peptide was interfering with transport activity, expression plasmids were made that produced a Myc peptide on the N-terminus of the proteins. As with the FLAG constructs, Myc-OCT1 and Myc-OCTN2 were functional in transporting MPP^+ or carnitine, respectively. However, Myc-BOCT1 and Myc-BOCT2 still failed to transport any of the tested substrates. BOCT1 and BOCT2 were expressed in other cell

Table 2 Uptake studies in stable recombinant HEK cell lines

Substrate	Uptake by transfectants (dpm/μg)				
	Vector	BOCT1	BOCT2	OCT1	OCTN2
MPP^+	9.3 ± 0.8	9.9 ± 0.7	9.0 ± 0.4	372 ± 12*	16.9 ± 0.4
TEA	117 ± 3.9	112 ± 1.7	126 ± 7.5	223 ± 6.4*	112 ± 7.2
Carnitine	186 ± 16	209 ± 6.1	192 ± 9.6	241 ± 6.7	2,288 ± 84*
Choline	271 ± 5.2	265 ± 7.0	272 ± 20	510 ± 8.8*	297 ± 47
Histamine	24.4 ± 7.7	9.1 ± 0.8	8.0 ± 1.1	95.7 ± 4.3*	nd
Norepinephrine	29.5 ± 1.1	35.2 ± 1.7	24.1 ± 1.0	159 ± 3.2*	nd
Nicotinamide	39.0 ± 10.9	32.1 ± 2.2	27.8 ± 5.1	130 ± 9.5*	nd
Urate	4.5 ± 1.5	7.4 ± 4.3	4.5 ± 0.13	4.6 ± 2.1	nd
Ascorbate	9.0 ± 2.1	10.1 ± 1.0	5.5 ± 0.3	6.5 ± 0.7	nd

nd not done

* Statistically significant from pFLAG vector, $P < 0.05$

lines to test if the lack of functional activity was a consequence of using HEK293 cells. However, as for HEK293 cells, no transport was observed when the BOCTs were expressed in 3T3, MC-IX-C or MDCK cells. Finally, to test if the unusual N-terminus in the BOCT proteins interfered with transport, we created chimeric proteins that replaced the N-terminus of BOCT1 and BOCT2 with the N-terminus of OCTN2. The fusion point in the chimeras was at the AFS sequence. The chimeric proteins were unable to transport carnitine or MPP^+ (data not shown). Thus, even though the critical protein core of the SLC22 family is present in BOCT1 and BOCT2, including conserved sequence elements, these proteins were unable to transport typical substrates for the SLC22 family.

Discussion

BOCT1 and BOCT2 are two novel rat SLC22 gene family members whose organic ion transport characteristics have not been previously reported. These genes have sequence homology to the organic cation transporter family, although there are unique characteristics of both BOCT1 and BOCT2 that diverge from other members of the family.

When this work was started, BOCT2 was identified in databases as a predicted gene product of 355 residues, assembled by gene prediction software and expressed sequence tags. After performing 5′ and 3′ RACE, we determined the nearly full-length mRNA sequence for this novel gene. The BOCT2 mRNA contains an unusual GC-rich region at the 5′ end. The initiator AUG actually exists within this GC-rich region, and it is preceded by two 23-bp inverted repeat sequences. When PCR was done across these regions, spontaneous deletions were obtained unless PCR was performed under GC-rich conditions. This indicates that this 5′UTR forms a stem loop or other secondary structure that impedes standard cDNA synthesis and PCR amplification. The presence of this secondary structure suggests that BOCT2 is subject to translational regulation. Still, BOCT2 was readily translated in HEK cells despite the presence of the 5′UTR. BOCT1 also has an atypical 5′UTR suggestive of translational regulation.

The tissue expression of BOCT1 and BOCT2 suggests a physiological role in brain. Both genes are also expressed in liver and kidney, a pattern that is common for organic ion transporters. In brain, both genes are present in capillary RNA where they could mediate entry into and/or efflux from the brain. BOCT1 is widely expressed in brain, including neurons, astrocytes, and choroid plexus. Expression in choroid plexus was the highest of any tissue examined and further supports an important function in brain homeostasis, although further data are needed to clarify this role. In contrast, BOCT2 was not expressed in choroid plexus, but was expressed in capillaries, as well as in neurons and astrocytes.

Despite sequence homology to the OCT family, BOCT1 and BOCT2 did not transport typical organic cations. The range of compounds tested included substrates for all known OCTs. In particular, known substrates for the most closely related transporters, OCT3 and ORCTL3 were not transported. We also tested substrates known to be transported at the choroid plexus. These novel proteins each possess a unique N-terminus that is unrelated to other SLC22 proteins, and it is possible that this unique structure explains the lack of transport activity. The fact that the BOCT1 cDNA was isolated from a blood–brain barrier cDNA library implies that the atypical N-terminus is a genuine feature of BOCT1 and is not an artifact of PCR or sequence manipulation. There is evidence that TM1 or certain residues in this segment are critical for transport activity [19]. However, others reported intact transport by alternatively spliced OCT1 lacking the first two TMDs [24]. Conserved sequence motifs for the SLC22 family are present in BOCT1 and BOCT2. However, chimeras containing the conserved sequences fused to the N-terminus of OCTN2 also failed to transport typical OCT substrates, suggesting the novel N-termini are not the critical determinant in inability to transport. We cannot rule out, at this time, that BOCT1 and BOCT2 could transport some other type of substrate that was not tested in this study. If they are transporters, they have a much narrower substrate specificity than other members of the SLC22 family. The evasiveness of the function of an orphan transporter is not unprecedented. A study of SLC7A4, a novel protein with high sequence homology to the subfamily of cationic amino acid transporters (CATs), failed to demonstrate any convincing transport activity [25]. It was proposed that despite its sequence homology, 7A4 is not an amino acid transporter or it requires additional proteins or factors to be functional. It is possible that BOCT1 and BOCT2 also require some type of cofactor to show functional activity. However, if this cofactor is required for function in HEK293, it is also absent in several other cell lines in which expression failed to elicit transport activity.

Another possible function for BOCT1 is that of a receptor. After beginning our studies, the mouse homolog of BOCT1 was cloned serendipitously after a search for proteins that conferred binding of the lipocalin, 24p3 (also known as lipocalin-2 [Lcn2]) [15]. It was shown that Lcn2 binds iron through a small molecular weight siderophore [26, 27], and mBOCT1 serves as a cell surface receptor (24p3R) for this lipocalin, allowing for iron uptake or apoptosis, depending on the iron content of the ligand [15]. Recently, human BOCT1 was cloned and proposed to act as a receptor for neutrophil gelatinase-associated lipocalin

(NGAL), the human ortholog of Lcn2. This function, however, has not yet been confirmed for the human protein [28]. Megalin was also shown to be a receptor for Lcn2 [29]. There are some discrepancies in previous studies in regards to the Lcn2 binding site on BOCT1. Devireddy et al. showed that 24p3 bound BOCT1 on the C-terminal end of the protein. One 24p3-interacting clone that was isolated consisted of only the last 74 amino acids of the protein. An alternate splice variant was cloned, called 24p3R-short, which lacked the N-terminal 154 amino acids. This short form actually showed higher affinity for 24p3 than the full-length protein [15]. In contrast, Fang et al. cloned a novel short form of human BOCT1 (NgalR-3) that lacked the C-terminal 313 amino acids. This group concluded that the N-terminal short form co-localized and was co-immunoprecipitated with human NGAL, although they could not show co-immunoprecipitation of NGAL with the full-length sequence of BOCT1 (NgalR-2) [28]. We were unable to show any binding of rat Lcn2 to rat BOCT1 using a variety of different methods including crosslinking, immunoprecipitation, flow cytometry, immunohistochemistry, and radioligand binding. With multiple splice forms and a disagreement about which region of the protein actually binds to Lcn2, it is difficult to conclusively assign the physiological function of BOCT1 as a receptor for Lcn2. However, if BOCT1 is a lipocalin receptor, it is reminiscent of STRA6 [30]. STRA6 is a multipass membrane receptor that mediates the uptake of retinol bound to the lipocalin, retinol binding protein. Endocytosis of the STRA6:RBP complex is not required for retinol uptake. It is possible that BOCT1 is a hybrid receptor/transporter in which this member of the SLC22 family has evolved to bind lipocalin through its novel amino terminus and transport lipocalin cargo through the conserved OCT domains. Future experiments will test this novel hypothesis.

Acknowledgments We would like to thank Laura Ngo, Kelly Fine, Jeff Smith, and Christi Srader for technical support. The authors would also like to thank Wesley M. Williams for assistance with microvessel purification. This research was funded by the National Institute of General Medical Sciences, [R15 GM070578] (JS) and the Achievement Rewards for College Scientists (ARCS) scholarship foundation (KMB).

References

1. Koepsell H, Lips K, Volk C (2007) Polyspecific organic cation transporters: structure, function, physiological roles, and biopharmaceutical implications. Pharm Res 24:1227–1251
2. Koepsell H, Busch A, Gorboulev V, Arndt P (1998) Structure and function of renal organic cation transporters. News Physiol Sci 13:11–16
3. Grundemann D, Gorboulev V, Gambaryan S, Veyhl M, Koepsell H (1994) Drug excretion mediated by a new prototype of polyspecific transporter. Nature 372:549–552
4. Zhang L, Dresser MJ, Gray AT, Yost SC, Terashita S, Giacomini KM (1997) Cloning and functional expression of a human liver organic cation transporter. Mol Pharmacol 51:913–921
5. Gorboulev V, Ulzheimer JC, Akhoundova A, Ulzheimer-Teuber I, Karbach U, Quester S, Baumann C, Lang F, Busch AE, Koepsell H (1997) Cloning and characterization of two human polyspecific organic cation transporters. DNA Cell Biol 16: 871–881
6. Green RM, Lo K, Sterritt C, Beier DR (1999) Cloning and functional expression of a mouse liver organic cation transporter. Hepatology 29:1556–1562
7. Okuda M, Saito H, Urakami Y, Takano M, Inui K (1996) cDNA cloning and functional expression of a novel rat kidney organic cation transporter, OCT2. Biochem Biophys Res Commun 224: 500–507
8. Mooslehner KA, Allen ND (1999) Cloning of the mouse organic cation transporter 2 gene, Slc22a2, from an enhancer-trap transgene integration locus. Mamm Genome 10:218–224
9. Enomoto A, Wempe MF, Tsuchida H, Shin HJ, Cha SH, Anzai N, Goto A, Sakamoto A, Niwa T, Kanai Y, Anders MW, Endou H (2002) Molecular identification of a novel carnitine transporter specific to human testis. Insights into the mechanism of carnitine recognition. J Biol Chem 277:36262–36271
10. Gong S, Lu X, Xu Y, Swiderski CF, Jordan CT, Moscow JA (2002) Identification of OCT6 as a novel organic cation transporter preferentially expressed in hematopoietic cells and leukemias. Exp Hematol 30:1162–1169
11. Jonker JW, Wagenaar E, Van Eijl S, Schinkel AH (2003) Deficiency in the organic cation transporters 1 and 2 (Oct1/Oct2 [Slc22a1/Slc22a2]) in mice abolishes renal secretion of organic cations. Mol Cell Biol 23:7902–7908
12. Wright SH (2005) Role of organic cation transporters in the renal handling of therapeutic agents and xenobiotics. Toxicol Appl Pharmacol 204:309–319
13. Strausberg RL, Feingold EA, Grouse LH et al (2002) Generation and initial analysis of more than 15,000 full-length human and mouse cDNA sequences. Proc Natl Acad Sci USA 99: 16899–16903
14. Jacobsson JA, Haitina T, Lindblom J, Fredriksson R (2007) Identification of six putative human transporters with structural similarity to the drug transporter SLC22 family. Genomics 90: 595–609
15. Devireddy LR, Gazin C, Zhu X, Green MR (2005) A cell-surface receptor for lipocalin 24p3 selectively mediates apoptosis and iron uptake. Cell 123:1293–1305
16. Williams WM, Reichman M, McNeill TH (1988) Cerebral microvascular and parenchymal phospholipid composition in the mouse. Neurochem Res 13:743–747
17. Maniatis T, Fritsch EF, Sambrook J (1982) Molecular cloning: a laboratory manual. Cold Spring Harbor Laboratory, New York
18. Bernsel A, Viklund H, Hennerdal A, Elofsson A (2009) TOPCONS: consensus prediction of membrane protein topology. Nucleic Acids Res 37:W465–W468
19. Burckhardt G, Wolff NA (2000) Structure of renal organic anion and cation transporters. Am J Physiol Renal Physiol 278:F853–F866
20. Gorboulev V, Shatskaya N, Volk C, Koepsell H (2005) Subtype-specific affinity for corticosterone of rat organic cation transporters rOCT1 and rOCT2 depends on three amino acids within the substrate binding region. Mol Pharmacol 67:1612–1619
21. Inazu M, Takeda H, Matsumiya T (2003) Expression and functional characterization of the extraneuronal monoamine transporter in normal human astrocytes. J Neurochem 84:43–52
22. Bahn A, Hagos Y, Reuter S, Balen D, Brzica H, Krick W, Burckhardt BC, Sabolic I, Burckhardt G (2008) Identification of a

new urate and high affinity nicotinate transporter, hOAT10 (SLC22A13). J Biol Chem 283:16332–16341
23. Spector R, Johanson C (2006) Micronutrient and urate transport in choroid plexus and kidney: implications for drug therapy. Pharm Res 23:2515–2524
24. Zhang L, Dresser MJ, Chun JK, Babbitt PC, Giacomini KM (1997) Cloning and functional characterization of a rat renal organic cation transporter isoform (rOCT1A). J Biol Chem 272:16548–16554
25. Wolf S, Janzen A, Vekony N, Martine U, Strand D, Closs EI (2002) Expression of solute carrier 7A4 (SLC7A4) in the plasma membrane is not sufficient to mediate amino acid transport activity. Biochem J 364:767–775
26. Goetz DH, Holmes MA, Borregaard N, Bluhm ME, Raymond KN, Strong RK (2002) The neutrophil lipocalin NGAL is a bacteriostatic agent that interferes with siderophore-mediated iron acquisition. Mol Cell 10:1033–1043
27. Yang J, Goetz D, Li JY, Wang W, Mori K, Setlik D, Du T, Erdjument-Bromage H, Tempst P, Strong R, Barasch J (2002) An iron delivery pathway mediated by a lipocalin. Mol Cell 10: 1045–1056
28. Fang WK, Xu LY, Lu XF, Liao LD, Cai WJ, Shen ZY, Li EM (2007) A novel alternative spliced variant of neutrophil gelatinase-associated lipocalin receptor in oesophageal carcinoma cells. Biochem J 403:297–303
29. Hvidberg V, Jacobsen C, Strong RK, Cowland JB, Moestrup SK, Borregaard N (2005) The endocytic receptor megalin binds the iron transporting neutrophil-gelatinase-associated lipocalin with high affinity and mediates its cellular uptake. FEBS Lett 579: 773–777
30. Kawaguchi R, Yu J, Honda J, Hu J, Whitelegge J, Ping P, Wiita P, Bok D, Sun H (2007) A membrane receptor for retinol binding protein mediates cellular uptake of vitamin A. Science 315: 820–825